A sinc-based approach for the solution of differential transport problems with periodic boundary conditions

P. Marconcini, D. Logoteta, and M. Macucci
Dipartimento di Ingegneria dell'Informazione, Università di Pisa, Via G. Caruso 16, I-56122 Pisa, Italy
e-mail: p.marconcini@iet.unipi.it

INTRODUCTION

A well-known method to solve a differential problem, and in particular a Schrödinger or Dirac transport equation, with periodic boundary conditions, is based on substituting each of the functions appearing in the differential system with its Fourier transform and solving the problem in terms of the Fourier coefficients of the unknown functions. A proper frequency cut-off has to be chosen to limit the size of the problem.

This approach is generally preferable to a direct real-space solution based on a finite-difference discretization scheme, since it avoids the errors related to the discretization of the derivatives. It can thus be shown that the precision of a solution found with the Fourier-space approach considering only N frequencies is generally better than that of a solution obtained with the direct-space finite-difference approach considering a grid of N points.

Here we discuss the possibility to obtain, working in the direct space, a method equivalent to that used in the reciprocal-space domain, and thus the same accuracy, using a particular set of basis functions in the solution of the problem.

METHOD AND RESULTS

The method is based on the use in the direct space of the following sampling functions for the quantities periodic with period $L = N\Delta$ (where Δ is the size of the considered direct-space mesh and N is the number of samples in the period):

$$g_\ell(x) = \sum_{\alpha=-\infty}^{\infty} \mathrm{sinc}\left(\frac{x-(\ell+\alpha N)\Delta}{\Delta}\right) \quad (1)$$

(where $\mathrm{sinc}(x) = \sin(\pi x)/(\pi x)$). In Fig. 1 we show an example of these basis functions for $N = 20$ and $\ell = 10$: it is clearly periodic with the same period L as the functions we are expanding.

In detail, assuming band-limited wave functions and potentials, we express them in terms of sinc functions using the sampling theorem and then, after some analytical elaborations, we find the correct expressions for all of the terms appearing in the transport equations, in the form of $g_\ell(x)$ function expansions. This allows us to obtain a direct space approach equivalent to that in the Fourier space and thus with the same accuracy properties.

As an example, we apply this method to solve the Dirac transport equation in an armchair graphene nanoribbon with the potential varying only in the transverse direction, which (as we have shown in [1], [2]) can be recast into a form with periodic boundary conditions. In particular, for the two transversal potentials represented in Fig. 2, we obtain the longitudinal wave vectors represented on the Gauss plane in Figs. 3 and 5, and, for the longitudinal wave vector with largest real part, the transverse envelope functions shown in Figs. 4 and 6. These results coincide with those obtained with the Fourier-space approach [1], [2] using a number of frequencies identical to the number of samples considered within the period in the direct-space domain.

REFERENCES

[1] P. Marconcini, D. Logoteta, M. Fagotti, M. Macucci, *Numerical solution of the Dirac equation for an armchair graphene nanoribbon in the presence of a transversally variable potential*, Proceedings of the 14th International Workshop on Computational Electronics, p. 53 (2010).

[2] M. Fagotti, C. Bonati, D. Logoteta, P. Marconcini, M. Macucci, *Armchair graphene nanoribbons: $\mathcal{PT}$-symmetry breaking and exceptional points without dissipation*, Phys. Rev. B **83**, 241406(R) (2011).

978-3-901578-26-7

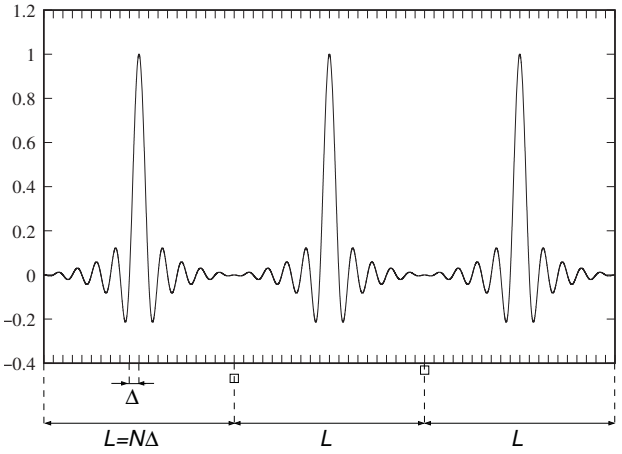

Fig. 1. Sinc basis function for $N = 20$ and $\ell = 10$ (three periods have been represented).

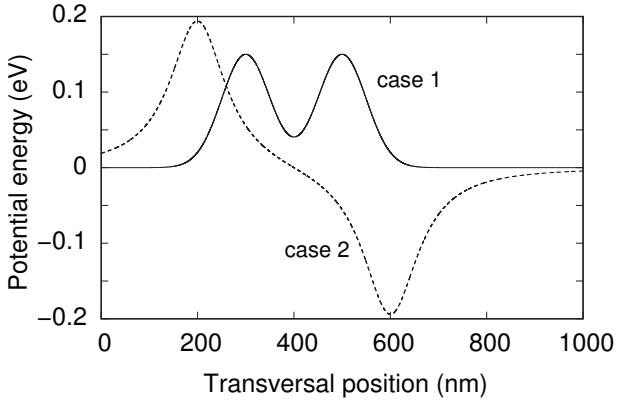

Fig. 2. The two transverse potentials for which the longitudinal wave vectors and transverse envelope functions of a 1 μm wide armchair nanoribbon have been computed using the sinc-based approach.

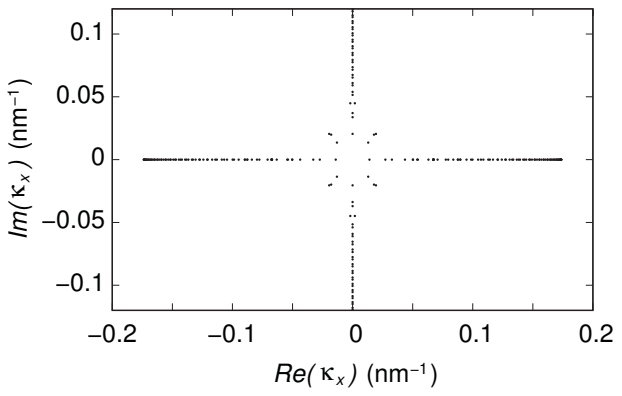

Fig. 3. Longitudinal wave vectors, represented on the Gauss plane, for the armchair nanoribbon in the presence of the potential of case 1 of Fig. 2.

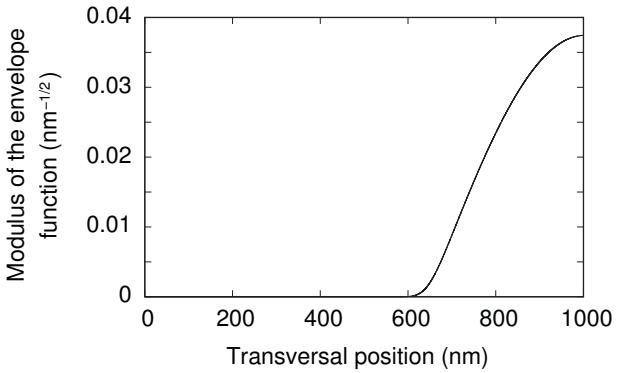

Fig. 4. Modulus of a transverse envelope function (corresponding to the longitudinal wave vector with largest real part) for the armchair nanoribbon in the presence of the potential of case 1 of Fig. 2.

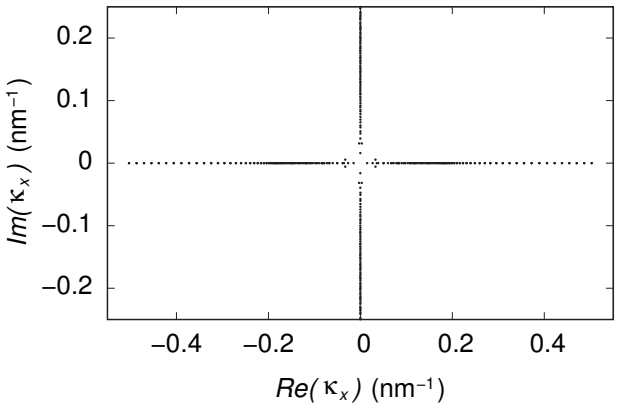

Fig. 5. Longitudinal wave vectors, represented on the Gauss plane, for the armchair nanoribbon in the presence of the potential of case 2 of Fig. 2.

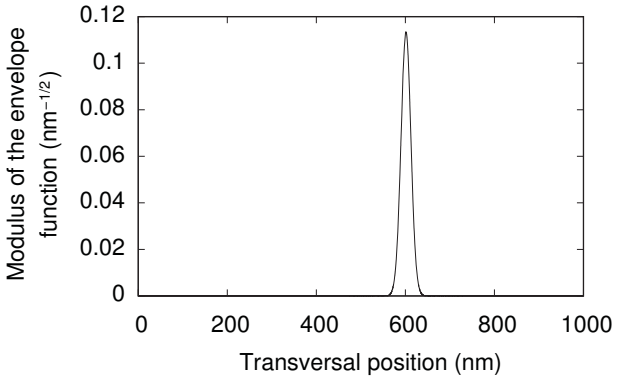

Fig. 6. Modulus of a transverse envelope function (corresponding to the longitudinal wave vector with largest real part) for the armchair nanoribbon in the presence of the potential of case 2 of Fig. 2.